



Published in final edited form as:

Otol Neurotol. 2015 April ; 36(4): 657–661. doi:10.1097/MAO.0000000000000573.

## Characterization of Intracochlear Rupture Forces in Fresh Human Cadaveric Cochleae

Daniel Schuster, MD<sup>1,\*</sup>, Louis B. Kratchman, BS<sup>2,\*</sup>, and Robert F. Labadie, MD, PhD<sup>1,3</sup>

<sup>1</sup>Department of Otolaryngology – Head and Neck Surgery, Vanderbilt University Medical Center, Nashville, TN

<sup>2</sup>Department of Mechanical Engineering, Vanderbilt University, Nashville, TN

<sup>3</sup>Department of Biomedical Engineering, Vanderbilt University, Nashville, TN

### Structured Abstract

**Hypothesis**—To develop a method to measure the forces required for a probe to translocate from scala tympani (ST) to scala vestibuli (SV) in fresh human cochleae.

**Background**—Translocation of cochlear implant (CI) electrodes from ST to SV may lead to suboptimal audiological outcomes. Prior work investigating the rupture forces of human intracochlear membranes comes from a single study conducted on isolated, *ex-vivo* cadaveric specimens.

**Methods**—Fresh (post mortem < 120 hours), non-fixed, never-frozen human temporal bones underwent preparation consisting of surgical isolation of the cochleae and exposure of the osseous spiral lamina (OSL), basilar membrane (BM), and Reissner's membrane (RM) complex by removing bone covering ST and SV. Each isolated cochlea was mounted to a force sensor using an adjustable mounting platform. A 300 μm diameter ball-tipped probe was attached to a piezoelectric linear motor and advanced at 1mm/sec from ST to SV while recording force from the load cell concurrent with video.

**Results**—Ten specimens were successfully exposed and analyzed. The range of rupture forces was 42 to 122 mN with a mean of 88 mN. Nine of the ten specimens failed via simple puncture while one failed by being avulsed from its medial attachment.

**Conclusions**—Using a novel technique we report the forces required to translocate a model of an electrode from the ST to the SV. Correlation to human perceptual ability is necessary to determine if a surgeon can detect such translocation during CI surgery.

### Introduction

Cochlear Implantation (CI) is the standard of care for severe to profound sensorineural hearing loss. Rapid progress in technology, from its inception in 1957 to FDA approval in

---

**Corresponding Author:** Robert F. Labadie, MD, PhD, 10269 Medical Center East, South Tower, Vanderbilt University Medical Center, Nashville, TN 37232-8606, robert.labadie@vanderbilt.edu, PHONE (615)-936-2493, FAX (615)-936-5515.

**Co-First Authors** – These two authors contributed equally to the work presented, including experimental design, data collection, data analysis, and manuscript preparation.

1984 to current multichannel devices with modern processing techniques, has led to a dramatic increase in the number of patients who have benefitted from this technology.<sup>1</sup> Despite overwhelming success, CI is not without complications. Estimates of complication rates in the literature range from 4–40%.<sup>2</sup> One major subset of complications involves problems associated with CI electrode insertion. In unusual cases, insertion of the electrode is not feasible due to anatomic considerations. In most other instances, electrode insertion is not perceived to be difficult but damage to intracochlear structures inadvertently occurs, potentially resulting in suboptimal hearing outcomes for patients.

The surgical technique for CI is typically via a standard mastoidectomy with facial recess approach to the middle ear. This is followed by entering the cochlea, either via the round window or a separate cochleostomy, and inserting an electrode array. The goal is to insert the array into the scala tympani (ST) without damage to intracochlear structures. One major challenge is poor visualization. The surgeon is able to visualize the cochleostomy itself, but intracochlear structures, such as the osseous spiral lamina (OSL), Reissner's membrane (RM), and the basilar membrane (BM), are only partially visible via the cochleostomy with the vast majority of the structure hidden by bone. The surgeon thus performs the critical step of the procedure blind to intracochlear anatomy and guided mainly by tactile feedback.

Translocation of the CI electrode array from ST to scala vestibuli (SV) with resultant intracochlear damage represents one cause of suboptimal hearing outcomes in patients undergoing CI. Multiple groups have documented poorer hearing outcomes should the electrode array cross from ST to SV.<sup>3,4,5</sup> Although data exists comparing histopathologic changes of the cochlea with varying insertion depths of CI electrodes,<sup>6</sup> there are limited data estimating the amount of force required for such translocation. The most relevant prior experimental results were reported by Ishii et. al, who used a blunt needle to puncture the round window (RW), basilar membrane (BM), and Reissner's membrane (RM), each of which was explanted from a single adult cochlea.<sup>7</sup> The authors reported a BM rupture force of approximately 30 millinewtons (mN). The single RM tested had a rupture force of 4.2 mN. We propose to treat the OSL, BM, and RM as one entity since most clinical translocations completely traverse from ST to SV, often involving damage to all three structures. In doing so we preserve the anatomical attachments of this group of structures, which we refer to collectively as the inter-scalar partition, to both the lateral and medial cochlear walls, which we hypothesize provide significant structural support. Additionally, we sought to develop a technique that could be used on multiple temporal bones in order to assess inter-specimen variability.

## Material and Methods

Twelve human temporal bones (6 left, 6 right) were acquired from a tissue harvesting service (Science Care, Phoenix, AZ). The temporal bones were harvested immediately post mortem, stored in saline, and shipped cooled, but not frozen. All experimentation was carried out with bones no greater than 120 hours post mortem.

Specimens were first prepared by isolating the cochlea without violating any intracochlear structures. This was achieved using the following dissection technique:

1. Perform a canal wall down mastoidectomy, including removal of the incus and malleus and sacrifice of the chorda tympani nerve.
2. Perform a labyrinthectomy.
3. Isolate the superior aspect of the cochlea by removing the horizontal (tympanic) segment of the facial nerve, and all bone superior to it with a 4 mm cutting drill bit.
4. Isolate the anterior aspect of the cochlea by drilling into the carotid artery, and removing all bone anterior to it.
5. Isolate the cochlea from bone posterior to it by drilling away the pyramidal eminence, sinus tympani, and vertical (mastoid) segment of the facial nerve.
6. Using hypotympanic air cells as an inferior landmark, cut away all remaining temporal bone with a diamond band saw (Gryphon Corp, Sylmar, CA), leaving an isolated cochlear specimen.

After the cochlea was isolated, a combination of micro-dissection instruments and 1mm diamond drill bit were used to manually expose the inter-scalar partition in the area approximately 90 degrees along the basal turn of the cochlea. Care was taken to leave labyrinthine bone in place between the round and oval windows as a supporting structure. Additionally, bone was left in place at the lateral cochlear wall. Bone overlying the ST and SV was removed under microscopy using a 1mm diamond bur to expose the inter-scalar partition from above and below (Figure 1).

The experimental apparatus (Figure 2) consisted of a custom-built rigid acrylic frame. A Nano-17 force sensor (ATI Industrial automation, Apex, North Carolina), was mounted to the base of the frame, and a small stage was attached to the force sensor to support cochlear specimens. The force sensor had a resolution of 1/320 N and was factory-calibrated immediately prior to the experiments. Each specimen was fixed with epoxy to a custom-built, adjustable mounting platform, which was placed on the stage. The platform was adjusted such that the surface of the inter-scalar partition that faces the ST was approximately orthogonal to the insertion axis, and then the mounting platform was locked by application of cyanoacrylate adhesive. In the experimental position, ST was immediately below the puncture probe and oriented above the SV. A SL-2060 piezoelectric linear motor with a displacement resolution of 1 micrometer (SmarAct GmbH, Oldenburg, Germany) was attached to the frame, and was used to advance a rigid probe with a 300  $\mu\text{m}$  diameter coordinate measurement machine ruby ball probe (itpstyli, St. Louis, MO), which was aligned with a single axis of the force sensor. With the aid of an operating microscope (Carl Zeiss AG, Oberkochen, Germany), the specimen was manually positioned directly underneath the tip of the probe, such that they were oriented orthogonal to the insertion axis. The probe was advanced until it was approximately 200  $\mu\text{m}$  from the tissue surface (Figures 3 & 4). The probe was then advanced at a velocity of 1 mm/sec from the ST to the SV while concurrently recording force from the load cell and video-microscopy of the rupture (Figure 5).

Custom software written in the C programming language was used to simultaneously control the motor and record data. The program was executed on a 2.66 GHz Intel Xeon processor

running an Ubuntu 12.04 Linux operating system that was configured for real time operation. The data was sampled at 5000 Hz, and filtered using a 5th-order zero-phase Butterworth filter with a cut-off frequency of 25 Hz. The peak puncture forces were estimated by calculating the absolute maximum value in each filtered data set. Additionally, each video was reviewed to determine the type of rupture that occurred. These were classified as either punctures or avulsions. A puncture was defined as the ruby ball penetrating from ST to SV without tissue detachment from lateral or medial support, while an avulsion was defined as a detachment from either the lateral or medial bony attachments without puncturing.

## Results

Twelve temporal bones were obtained and prepared. A total of 10 bones were included in the final analysis. One of the excluded specimens was damaged during preparation, and was not analyzed due to its lack of structural integrity at the time of testing. In the second excluded specimen, the probe was inadvertently advanced into the labyrinthine bone below the SV during experimentation, causing a very large spike in force measurements from which we were unable to isolate the rupture forces. Consequently, this specimen was excluded from final analysis.

Nine of the ten specimens demonstrated an approximately linear increase in force, followed by a rapid release of force noted immediately after puncture of an elastic surface (Figure 6). In one specimen, an avulsion from the medial wall occurred. The rupture forces ranged from a minimum of 42 to a maximum of 122 mN, with a mean of 88 mN and a sample standard deviation of 25 mN.

## Discussion

Our measurements of the forces required to translocate a test probe from the ST to the SV have significant clinical implications regarding CI surgery. Our test probe results are comparable to translocation of electrode arrays. This represents perhaps the largest avoidable cause of failure to maintain residual hearing, which has been shown to impact audiological outcomes even in patients with little to no serviceable pre-operative hearing<sup>8</sup>. Prior to the work presented herein, there were few published results from which to estimate unsafe forces during CI electrode array insertion. This information is useful as systems and techniques for CI electrode array insertion are refined, including robotic systems which could be programmed to insert electrodes up to a given force level below which intracochlear trauma would be unlikely to occur.

To our knowledge, this is the first report of measured rupture forces associated with translocation from ST to SV in-situ (i.e. tissues left attached to their native bony attachments). While Ishii et. al have previously performed experimentation to calculate the mechanical properties of isolated human BM tissue<sup>7</sup>, these experiments evaluated a single fixed and explanted specimen, divided into 3 separate samples from different regions of the cochlea. This tissue lacked the in-vivo support that would resist the forces applied by an electrode during CI surgery, as it was fixed and explanted. To overcome this limitation, we

have developed a novel method of cochlear preparation in which the OSL, BM, and RM of the cochlea are exposed approximately 90 degrees along the basal turn, while maintaining attachments to the medial and lateral cochlear walls. Additionally, we performed the experiments on a larger sample size (n=10). The mean rupture force was 88 mN, supporting our hypothesis that the OSL, BM, and RM complex, complete with native lateral and medial attachments, would have a larger rupture force than *ex-vivo* BM as tested in the 1995 study.<sup>7</sup>

The experimental setup was designed to replicate the conditions relevant to puncture of the inter-scalar partition. One aspect of this was the choice of the indenter used. The diameter of the ruby ball-tipped indenter was 300  $\mu\text{m}$ , which is similar in size to that of a CI electrode array tip. Additionally, its rounded shape eliminates the sharp edge used in prior work<sup>7</sup>, which could cut tissue, potentially falsely reducing the forces necessary to rupture it. The hard spherical indenter also provides a well-defined contact condition for each trial. To mimic the in-vivo tissue as closely as possible, we used fresh, less than 120 hours post-mortem, tissue that was not fixed and had never been frozen. In addition, we developed a method of exposing the OSL, BM and RM complex approximately 90 degrees along the basal turn from both ST and SV without disrupting its native bony attachments, allowing us to closely simulate the clinical scenario of CI.

Although the work described here represents an important step in obtaining a better understanding of clinically relevant intracochlear trauma, more work is necessary to further characterize it. Our work investigated normal forces (i.e., those perpendicular to the inter-scalar partition) exclusively, in order to faithfully replicate the rupture phenomenon and to characterize one fundamental type of loading. It is hypothesized that clinical damage often occurs when the electrode array is deflected off the walls of scala tympani in the basal turn, approximately 180 degrees from the insertion site, during which we believe normal forces predominate. However, over the full length of insertion, punctures may occur at various angles to the inter-scalar partition, and understanding of the mechanisms of trauma may be improved by investigation of combined normal and tangential loading at different locations along the cochlea in the future.

As CI surgical techniques continue to improve, automated electrode insertion may hold the potential to minimize trauma by inserting at a slow, regulated velocity and stopping or altering the insertion trajectory when a real time force feedback indicates forces high enough to cause trauma, e.g. translocation from ST to SV. Our group has studied robotic insertion and have shown that electrodes inserted robotically have significantly less variation in force than those inserted by human operators.<sup>9</sup> Furthermore, preliminary data on electrode insertion forces generated during robotic insertion demonstrate significant differences between standard insertion techniques and those guided by stylets to avoid collision with the cochlear walls.<sup>10</sup> Prior to the work described herein, the clinical significance of these findings were speculative at best. We conclude that minimizing insertion forces will reduce the risk of translocation of a CI electrode array, and lead to improved audiological outcomes. Our data suggests an average of 88 mN is required for such translocation to occur, but they can occur with forces as low as 42 mN. This leads to perhaps the most perplexing question generated by these data – can human surgeons perceive and react to

such force levels? This represents an area of future research, which will be necessary in order to accurately compare traditional to robotic insertion techniques.

## Acknowledgments

The authors wish to acknowledge C. Gary Wright, PhD for his help in interpreting intracochlear anatomy and Jennifer Best, MD for her artistic talent and provision of the cochlear schematic.

**Funding Source:** This work was supported by Award Number R01DC010184 (RFL) from the National Institute On Deafness And Other Communication Disorders. The content is solely the responsibility of the authors and does not necessarily represent the official views of the National Institute On Deafness And Other Communication Disorders or the National Institutes of Health.

## References

1. Mangus B, Rivas A, Tsai BS, et al. Surgical techniques in cochlear implants. *Otolaryngol Clin N Am.* 2012; 45:69–80.
2. Brito R, Monteiro TA, Leal AF, et al. Surgical complications in 550 consecutive cochlear implantation. *Braz J Otorhinolaryngol.* 2012; 78(3):80–5. [PubMed: 22714851]
3. Aschendorf A, Kromeier J, Klenzner T, Laszig R. Quality control after insertion of the Nucleus Contour and Contour Advance Electrode in Adults. *Ear & Hearing.* 2007; 28:75S–79S. [PubMed: 17496653]
4. Skinner MW, Holden TA, Whiting BR, Voie AH, Brunsdon B, Neely JH, Saxon EA, Hullar TE, Finley CC. In vivo estimates of the position of Advanced Bionics electrode arrays in the human cochlea. *Annals of Otology, Rhinology & Laryngology.* 116((4)Suppl 197):1–24.
5. Finley CC, Holden TA, Holden LK, Whiting BR, Chole RA, Neely GJ, Hullar TE, Skinner MW. Role of electrode placement as a contributor to variability in cochlear implant outcomes. *Otol Neurotol.* 2008 Oct; 29(7):920–8. [PubMed: 18667935]
6. Adunka O, Kiefer J. Impact of electrode insertion depth on intracochlear trauma. *Otolaryngol Head Neck Surg.* 2006; 135:374–382. [PubMed: 16949967]
7. Ishii T, Takayama M, Takahashi Y. Mechanical properties of human round window, basilar and Reissner's membrane. *Acta Otolaryngol (stockh).* 1995; (Suppl 519):78–82.
8. Carlson ML, Driscoll CL, Gifford RH, et al. Implications of minimizing trauma during conventional cochlear implantation. *Otol Neurotol.* 2011; 32:962–968. [PubMed: 21659922]
9. Majdani O, Schurzig D, Hussong A, Rau T, Wittkopf J, Lenarz T, Labadie RF. Force Measurement of Insertion of Cochlear Implant Electrode Arrays in-vitro: Comparison of Surgeon to Automated Insertion Tool. *Acta Oto-Laryngologica.* Jan; 2010 130(1):31–36. [PubMed: 19484593]
10. Schurzig D, Webster RJ, Dietrich MS, et al. Force of cochlear implant electrode insertion performed by a robotic insertion tool: comparison of traditional versus advance off-stylet techniques. *Otol Neurotol.* 2010; 31:1207–1210. [PubMed: 20814345]

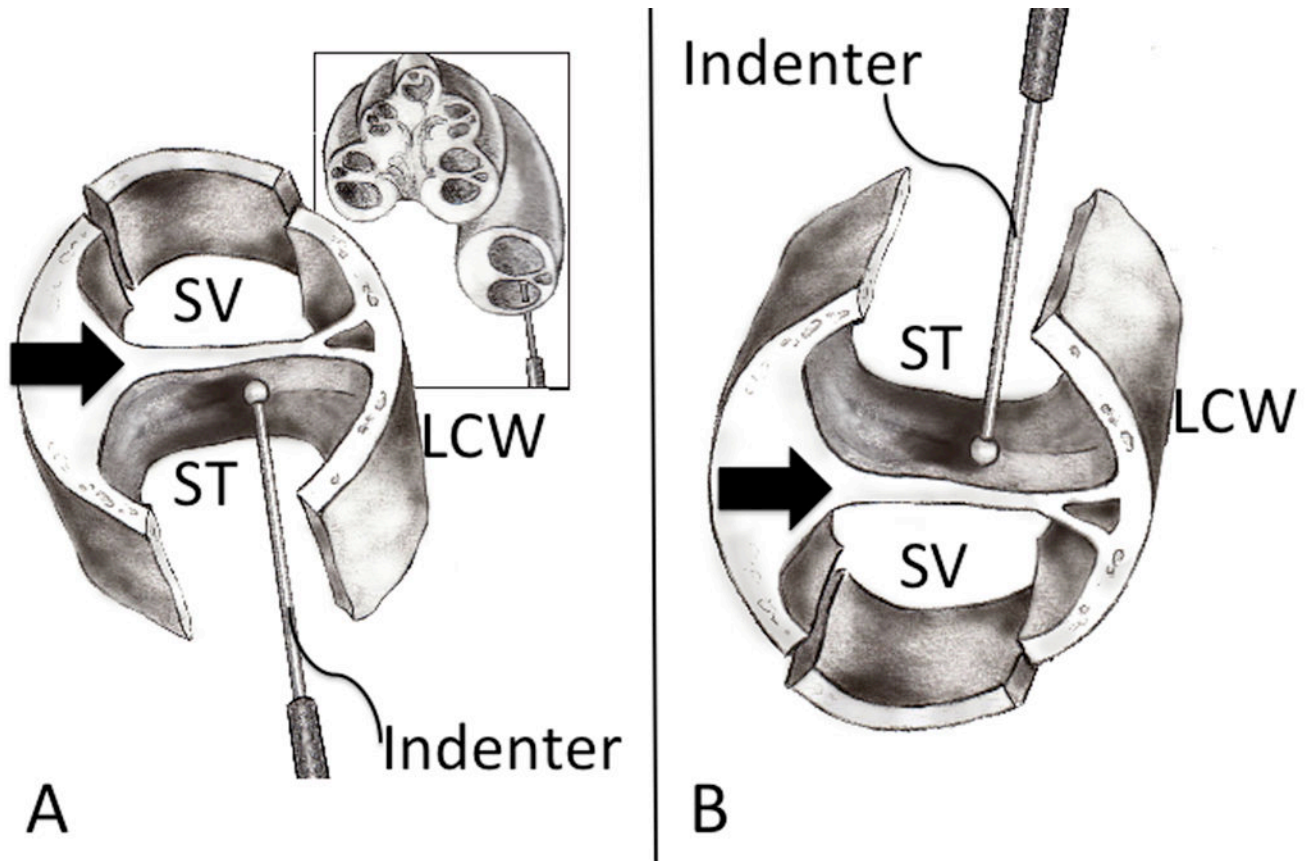


**Figure 1. Cochlear Schematic**

(A) A schematic cross section of a right cochlea, with an indenter probe entering the scala tympani approximately 90 degrees along the basal turn. The schematic in the foreground shows the inter-scalar partition (black arrow) exposed from below (bone underlying ST has been drilled away) and above (removal of bone overlying the SV is shown). LCW – lateral cochlear wall. (B) Orientation of cochlear specimen used during experimentation, which is upside-down (flipped 180 degrees) from anatomic orientation, such that ST is above SV.

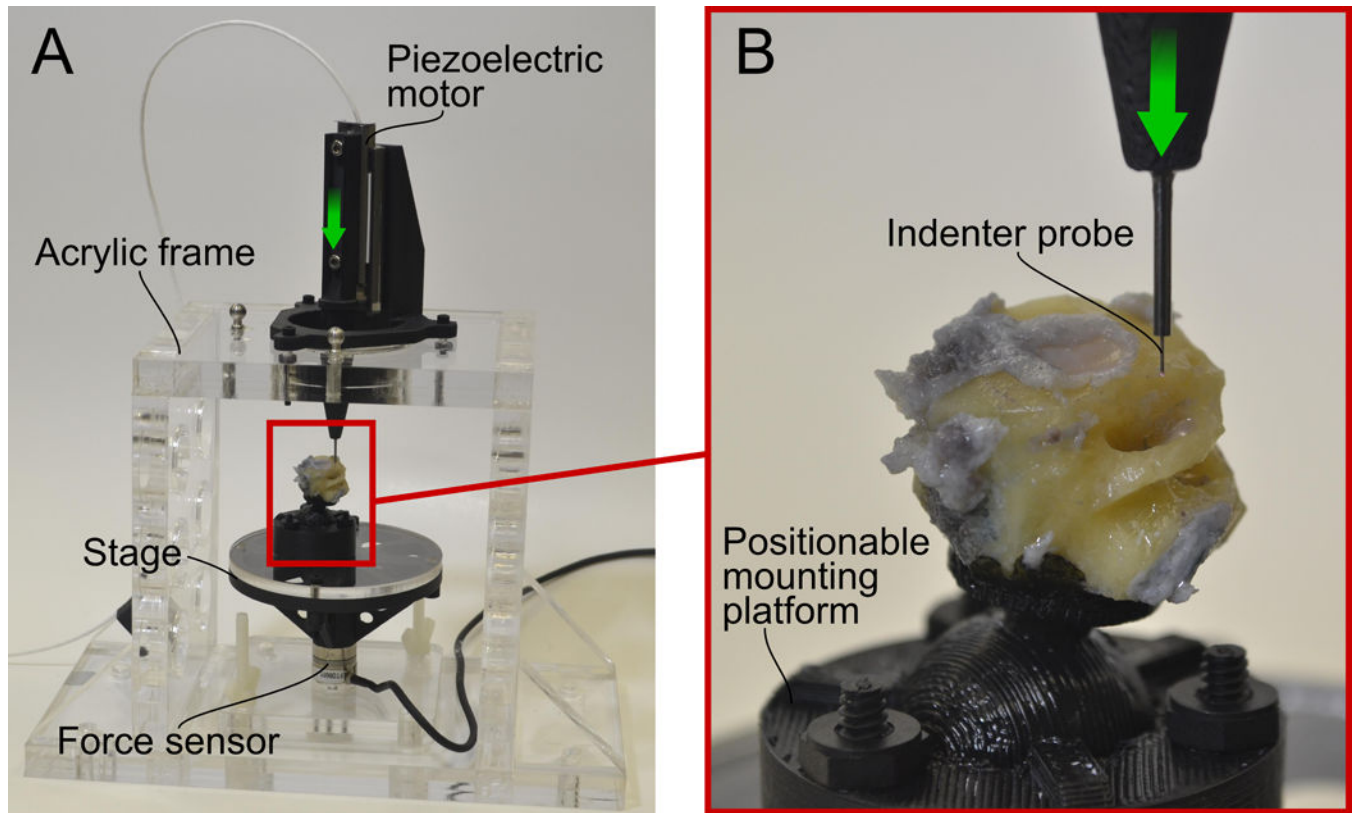


**Figure 2. Experimental Apparatus**

(A) A sturdy acrylic frame supports a force sensor and piezoelectric motor. The piezoelectric motor advances in the direction of the arrow to contact the specimen, which rests on a stage attached to the force sensor. (B) An enlarged view of the indenter, which is tipped with a 300  $\mu\text{m}$  diameter ruby sphere. The positionable mounting platform allows the specimen to be oriented such that the scala tympani is positioned just below the probe, with the BM, OSL, and RM approximately perpendicular to the insertion axis.



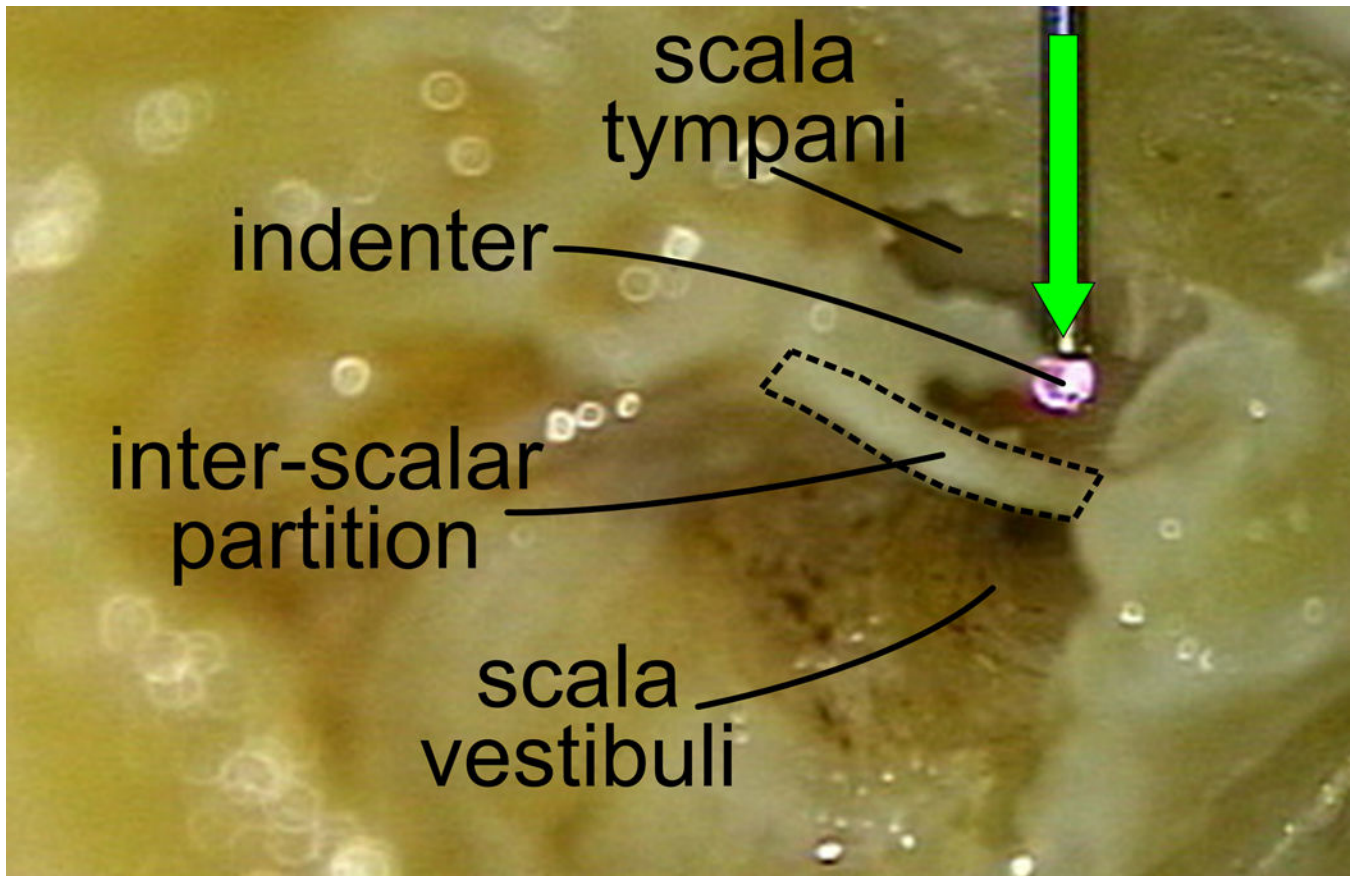


**Figure 3. Orientation of experimental setup**

Left cochlear specimen showing orientation of indenter to the inter-scalar partition prior to rupture. Bone between round and oval windows in this specimen has been removed to demonstrate the anatomy (pilot experiments, not included in data collection or analysis). The inter-scalar partition can be seen dividing the cochlear chambers into scala tympani above, and scala vestibuli below. The indenter moves in the direction of the green arrow.

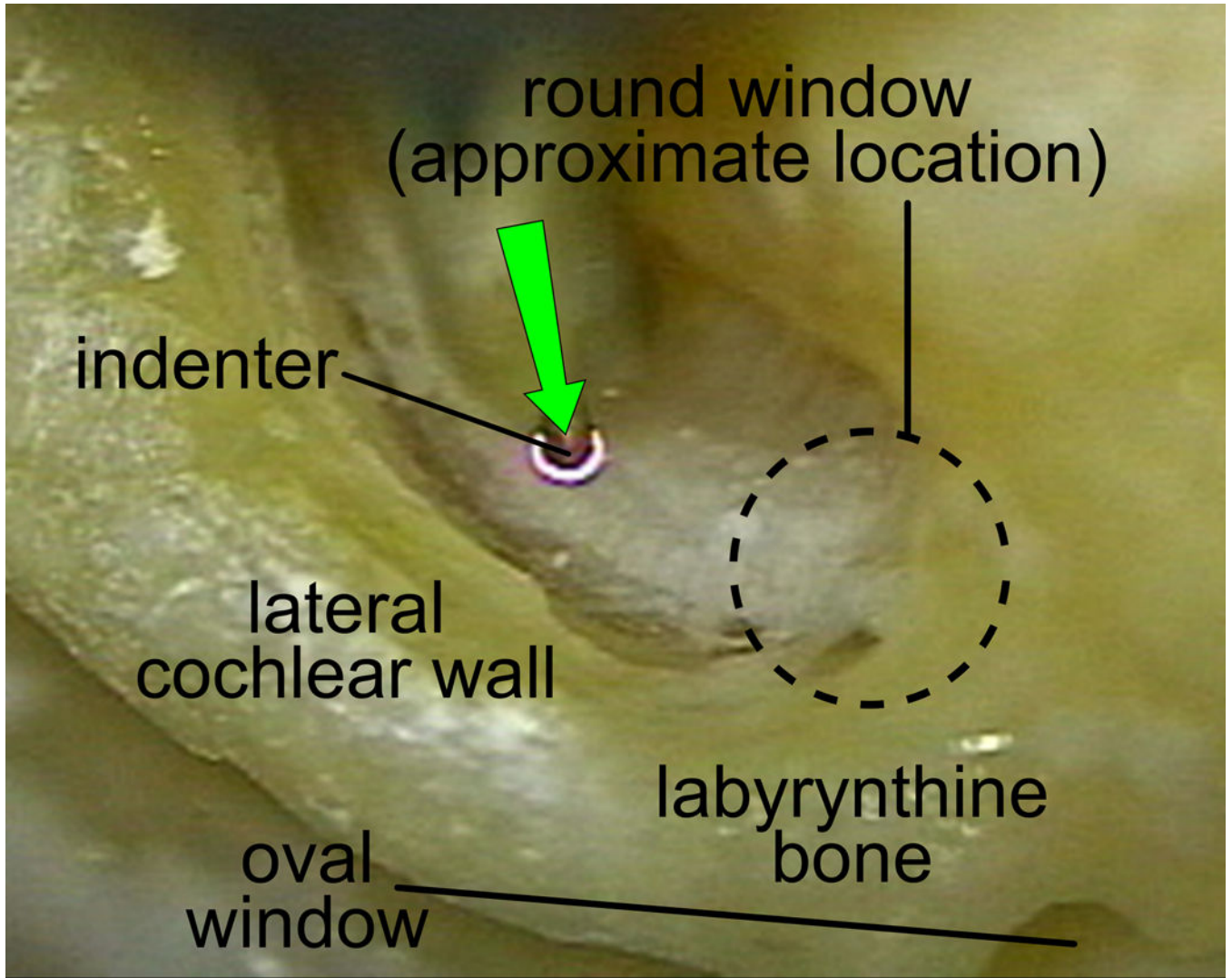


**Figure 4. Right fresh human cochlear specimen before rupture, viewed from scala tympani**  
 The indenter is positioned directly above the inter-scalar partition, which is supported by native bony attachments. The dashed line indicates the approximate RW region prior to removing the RW niche and RW membrane.

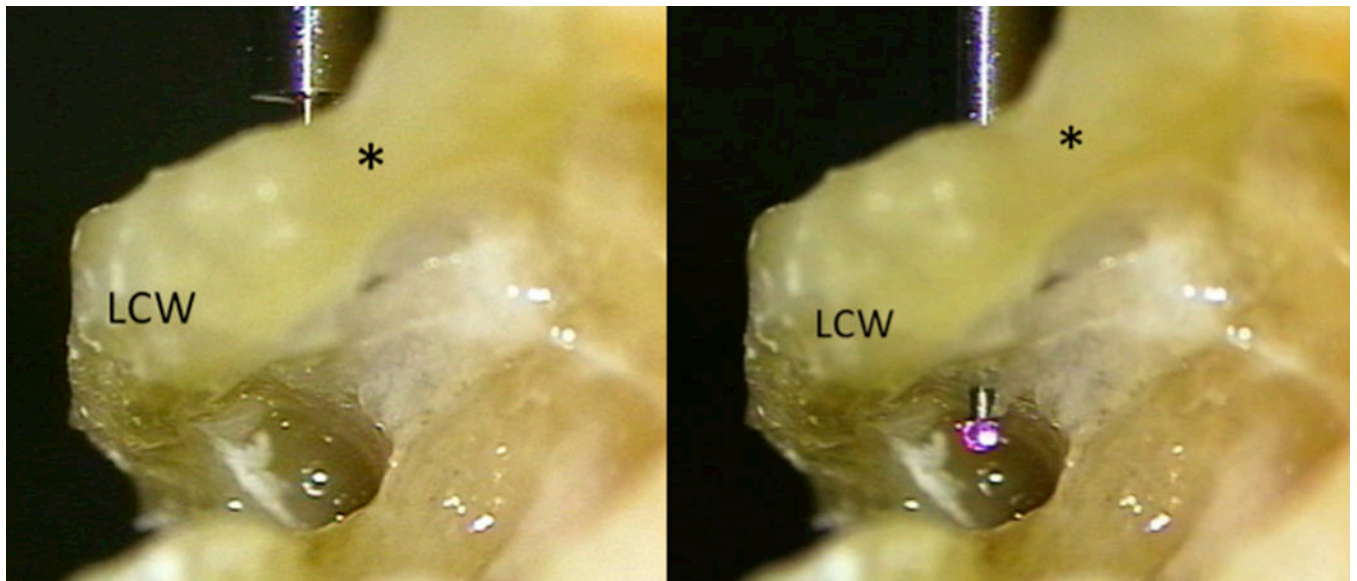


**Figure 5. Right fresh human inter-scalar partition before and after rupture, viewed from scala vestibuli**

Pre-rupture (left) and post-rupture (right) view of the specimen. The bony structural support can be seen on either side of the inter-scalar partition (LCW = Lateral Cochlear Wall). The asterisk denotes labyrinthine bone between the round and oval windows. Note that the ruby ball punctures the inter-scalar partition without detaching it from the surrounding bone.

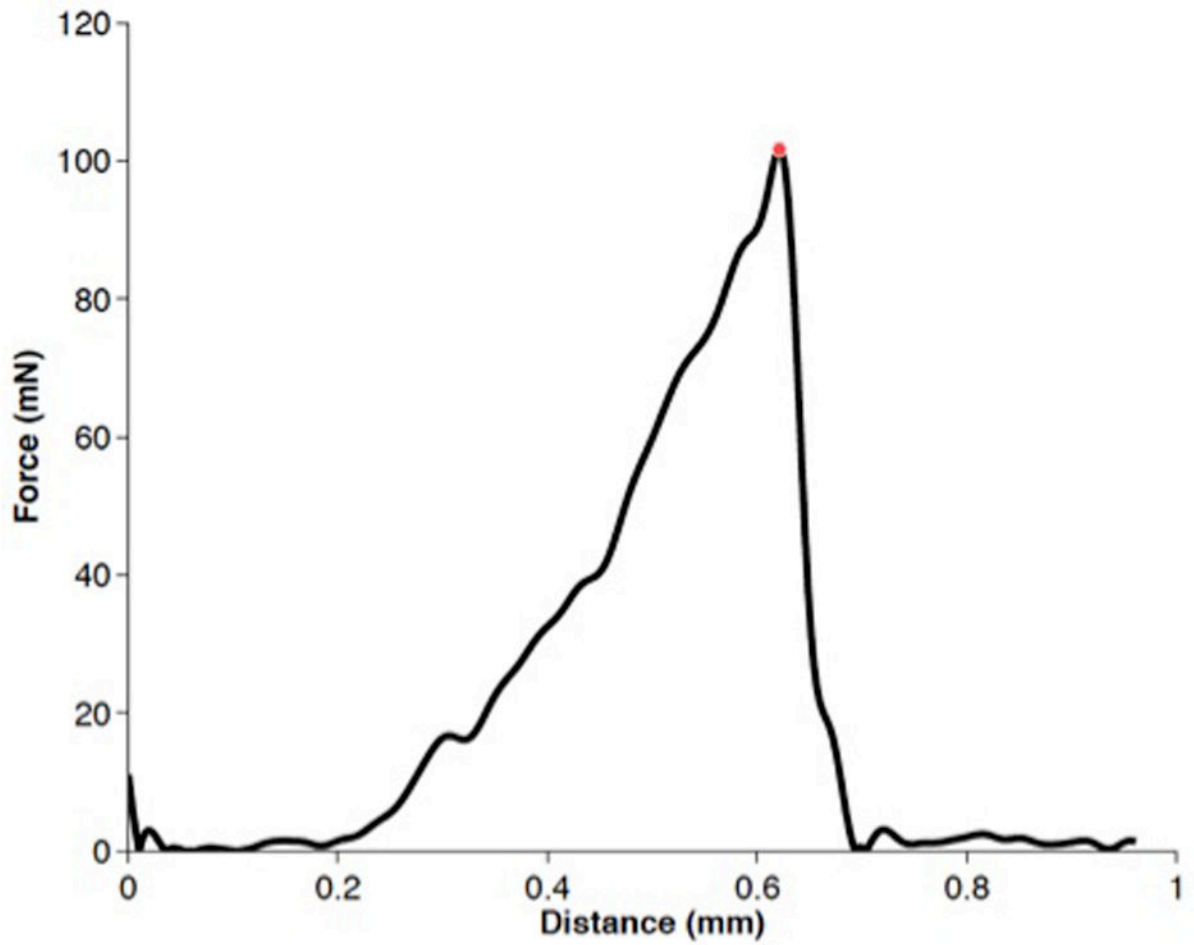


**Figure 6. Representative plot of inter-scalar partition rupture**

The recorded force increases as the indenter causes displacement of the complex. As rupture occurs, there is a rapid release of strain energy. The red dot represents the force at rupture for this trial.